Experimental Hematology

Experimental Hematology 2019;72:36–46

Compounds targeting class II histone deacetylases do not cause panHDACI-associated impairment of megakaryocyte differentiation

Damir Simic[a,b], and Nianli Sang[a,c]

[a]*Department of Biology, Drexel University, Philadelphia, PA;* [b]*Janssen R&D, Preclinical Development & Safety, Johnson & Johnson, Spring House, PA, USA;* [c]*Sidney Kimmel Cancer Center, Philadelphia, PA*

(Received 25 September 2018; revised 27 December 2018; accepted 28 December 2018)

Histone deacetylase inhibitors (HDACIs) have demonstrated effectiveness against lymphomas and myelomas in clinical practice. However, common to all currently approved broad-acting HDACIs (panHDACIs) is dose-limiting thrombocytopenia, which has prevented wider use in cancer therapy. Using $CD34^+$ hematopoietic stem cells (HSCs), we show that megakaryocyte (MK) cell maturation and differentiation are impaired by panHDACIs, correlating to clinical thrombocytopenia. Importantly, we demonstrate that inhibitors of class II histone deacetylases (HDACs), including LMK235 and tubacin at clinically relevant concentrations, do not affect MK maturation. Furthermore, we show that HDACI-induced impairment of MK differentiation is associated with reduction of protein levels of the transcription factor GATA-1, but not tubulin hyperacetylation. Finally, we report that panHDACIs trigger a rapid loss of GATA-1 protein via a proteasome-dependent pathway. Our data support the notion that specifically targeting class II HDACs in cancer treatment is a potential strategy that would offer a safer alternative than current panHDACIs.

The first generation of histone deacetylase inhibitors (HDACIs) has shown significant efficacy in the inhibition of cancer cell proliferation both in in vitro and in xenograft in vivo models. These inhibitors are generally broad acting (pan), inhibiting a number of histone deacetylases (HDACs) with increasing class preference depending on the concentration. Currently, four panHDACIs—suberoyl anilide hydroxamic acid (SAHA), panobinostat, romidepsin, and belinostat—have been approved by the Food and Drug Administration as epigenetic therapies, mainly for the treatment of T-cell lymphomas and multiple myelomas. However, clinical panHDACIs are limited by serious adverse effects, most notably thrombocytopenia, which is often dose limiting [1,2]. Limiting dosing restricts the effectiveness and broader use of panHDACIs as anticancer agents. Identifying specific members of HDACs as cancer therapeutic targets would allow for the development of a new generation of HDACIs to minimize the risk of thrombocytopenia.

Several reports suggest that the impairment of megakaryocyte (MK) maturation is the cause of panHDACI-induced thrombocytopenia. Preclinical models show that panHDACIs cause no change in serum thrombopoietin level or platelet and bone marrow toxicity, but lead to elevated immature MKs in spleen and bone marrow [3]. The panHDACI-induced impairment of megakaryopoiesis has been correlated with tubulin hyperacetylation and loss of GATA-1 function [3–5]. However, the underlying molecular mechanisms remain unclear.

Using in vitro HSC cell differentiation to MKs as a model of megakaryopoiesis, we compared the effects of current panHDACIs versus specific inhibitors targeting HDAC4, HDAC5, and HDAC6 on hematopoietic stem cells (HSCs; $CD34^+$). In addition, using both primary and cell line models, we further explored the role of GATA-1 loss in MK cell maturation, as well as the underlying mechanisms. We provide convincing data to demonstrate that LMK235, an HDAC5 (half-maximal inhibitory concentration [IC_{50}] = 4 nmol/L) and HDAC4 (IC_{50} = 12 nmol/L) inhibitor, does not affect MK maturation or protein levels of GATA-1 at biologically relevant concentrations. We also show that tubacin, an established HDAC6-specific inhibitor (IC_{50} = 4 nmol/L) that causes profound tubulin hyperacetylation, had no effect on GATA-1 levels

Offprint requests to: Dr. Nianli Sang, Biology, Pathology and Lab Medicine, 3245 Chestnut St, PISB 417, Drexel University, Philadelphia, PA 19104;; E-mail: nianli.sang@drexel.edu

0301-472X/
https://doi.org/10.1016/j.exphem.2018.12.007

or MK maturation. These data support the notion that specifically targeting members of class II HDACs such as HDAC4, HDAC5, and HDAC6 as cancer therapy may potentially avoid the thrombocytopenia caused by pan-HDACIs.

Methods

Cell culture, differentiation, and proliferation assays

Human $CD34^+$ HSCs (mixed donor) were purchased from Stem Cell Technologies (catalog #70008, Vancouver, Canada) and expanded in StemSpan SFEM II medium (catalog #09605) supplemented with StemSpan MK expansion supplement (catalog #02696; both from Stem Cell Technologies) to induce differentiation. To differentiate MKs, 3,000 $CD34^+$ cells were plated in 100 μL per well of a 96-well dish of the complete culture medium (StemSpan SFEMII medium supplemented with StemSpan CC220). Cells were incubated in humidified 5% CO_2/95% air atmosphere at 37°C for 7 days. After 7 days of culture, each well was filled with 100 μL of fresh complete culture medium. At day 14, cells were processed for flow cytometry analysis. Imaging was conducted using a Zeiss Axiovert 25 and Axiocam 503 mono camera. $CD34^+$ cells were imaged in 96-well plates using a 40 × objective. Total cells were counted using a hemocytometer.

Meg-01 cells were purchased from the American Type Culture Collection (Manassas, VA) and grown in RPMI 1640 medium containing 2 mmol/L glutamine, 10 mmol/L HEPES, 1 mmol/L sodium pyruvate, and 4500 mg/L sodium bicarbonate supplemented with 10% fetal bovine serum (FBS) and 1% penicillin/streptomycin. All cell culture reagents were purchased from Sigma-Aldrich (St. Louis, MO) unless stated otherwise.

The human ovarian carcinoma cell line A2780 was purchased from Sigma-Aldrich and grown in Eagle's minimum essential medium containing 2 mmol/L glutamine, 1 mmol/L sodium pyruvate, and 1500 mg/L sodium bicarbonate supplemented with 10% FBS and 1% penicillin/streptomycin. Proliferation was assessed using a CyQUANT cell proliferation kit (Thermo Fisher Scientific, Waltham, MA).

Special compounds, agents, and cell treatment

LMK235 (catalog #4830), SAHA (catalog #4652), and tubacin (catalog #3402) were from Tocris Bioscience (Minneapolis, MN). Panobinostat (catalog #A8178) was from ApexBio (Houston, TX). MG132 (catalog #101760-492) was from Selleck Chemicals (Houston, TX). All cell dimethylsulfoxide (DMSO) control treatments contained ≤0.1% DMSO.

Western blotting assays

Western blotting reagents were purchased from Thermo Fisher Scientific unless stated otherwise. Cells were lysed in M-Per mammalian protein extraction reagent (catalog #78501) supplemented with the Halt protease and phosphatase inhibitor cocktail following the manufacturer's instructions. Quantification of total protein was achieved with a bicinchoninic acid assay. For each sample, 20–40 μg of protein was separated by electrophoresis using 12% Tris-glycine gels. Protein transfers were performed using the iBlot2 system (20V for 1 min, 23V for 3 min, and 25V for 2 min). Polyvinylidene fluoride membranes were blocked in 4% milk-Tris buffered saline with Tween 20 buffer for 1 hour and incubated in primary antibody overnight, followed by the horseradish peroxidase (HRP) secondary antibody for 1 hour.

The primary antibodies used were: GATA-1 (Abcam; catalog #89505, mouse monoclonal), acetylated tubulin (Santa Cruz Biotechnology, Dallas, TX; catalog #sc-23950, mouse monoclonal), alpha tubulin (Abcam; catalog #4074, rabbit polyclonal), histone 3 (H3; ProSci, Poway, CA; catalog #31-007), and acetylated H3 (Thermo Fisher Scientific; Lys6, catalog #MA5-11195 and Lys36, catalog #MA-24672). Secondary HRP-labeled, anti-mouse (catalog #6728) and antirabbit (catalog #6721) antibodies were from Abcam. Membranes were incubated for 1 min in enhanced chemiluminescence reagent and captured using ChemiDoc MP (Bio-Rad, Hercules, CA).

Flow cytometry

Differentiated MKs were centrifuged (five wells of a 96-well dish were pooled) for 10 min at 800 *g* and washed twice in phosphate-buffered saline. The cells were then resuspended in 100 μL of staining buffer (catalog #420201; BioLegend, San Diego, CA) to which 5 μL of 7-amino-actinomycin D (7-AAD; Thermo Fisher Scientific), 20 μL of fluorescein isothiocyanate-conjugated anti-CD41 (Becton-Dickinson, Mountain View, CA), and 20 μL of phycoerythrin (PE)-conjugated anti-CD42b (GP1BA) antibodies (Becton-Dickinson) were added and incubated for 20 min at room temperature. The fraction of 7-AAD-positive cells (nonviable cells) was excluded from the analysis. Anti-CD41 and anti-CD42b were used to label total differentiating MK and mature MKs, respectively. Scatter plots and MK maturity dot plots represent data generated from the same well and sample. Ploidy was generated from the adjacent duplicate wells to avoid propidium iodide (PI) and PE (anti-CD42b) interference. Ploidy evaluation studies were modified from previously published protocols [6,7]. Briefly, cells were fixed overnight at 4°C in 100% ethanol, followed by the DNA staining with 0.05 mg/mL PI for 20 min in the dark. Data were acquired using an LSR Fortessa flow cytometer and analyzed using FACSDiva software (Becton-Dickinson) and FlowJo software (Ashland, OR). All experiments were repeated at least three times.

Quantitative reverse transcriptase polymerase chain reaction

For quantitative reverse transcriptase polymerase chain reaction (qRT-PCR), total RNA was isolated using the RNeasy kit (Qiagen, Germantown, MD). The RT reaction was performed using SuperScript VILO master mix (Thermo Fisher Scientific) to generate cDNA. PCR was performed using TaqMan Universal PCR master mixture with a ViiA 7 real-time PCR system (Thermo Fisher Scientific). All primers and probes were from Thermo Fisher Scientific.

Data analysis

Graphs and statistical analyses were generated using GraphPad Prism software version 7 (La Jolla, CA). Mean values were considered statistically significant at $p < 0.05$.

Results

Targeted inhibition of HDAC4 and HDAC5 does not impair MK differentiation

To determine whether specifically inhibiting HDAC4 and HDAC5 has an effect on MK maturation, we induced human HSCs ($CD34^+$ primary cells) to differentiate to mature MKs by following established procedures in the presence or absence of pharmacologically equivalent concentrations of LMK235, SAHA, and panobinostat [5,8]. Relevant testing concentrations of panHDACIs (SAHA and panobinostat), were established using respective maximum clinical serum concentration (C_{max}) values as a reference. LMK235 was tested at concentrations sufficient to increase α-tubulin acetylation, a known HDAC5 substrate [9]. In addition, the concentrations tested were 25–40 times that of enzymatic IC_{50}. After 14 days of directional induction, we characterized and quantitated the cell population using fluorescence-activated cell sorting analyses and light microscopy. Treating HSC cells with LMK235 (at ≤200 nmol/L) had no apparent negative effects on MK differentiation and maturation, as noted by the cell morphology dot plots and numbers of mature MKs (Figure 1A, top and middle rows, respectively). Two distinct populations (P1 and P2) of high-scatter cells were identified and P2 was further characterized as mature MK ($CD42b^+/CD41^+$), whereas P1 was mainly $CD42b^{low}/CD41^{low}$, thus representing undifferentiated cells. In contrast, panobinostat had a significant impact on MK maturation, with most of the HSC cells remaining undifferentiated ($CD42b^{low}/CD41^{low}$). Consistent with previous reports, panobinostat as low as 5 nmol/L significantly decreased the numbers of mature MKs ($CD42b^+/CD41^+$) from 44% (control) to 12% (Figure 1B). Treatment with SAHA at 500 nmol/L also caused a reduction in MK maturation (from 44% to 20%). When tested at or slightly below their clinical C_{max} concentrations, both SAHA and panobinostat resulted in a >50% reduction in mature MKs, consistent with the high frequency of thrombocytopenias reported in clinical cancer treatment [10,11]. Interestingly, despite the low number of MK mature cells, panobinostat and SAHA treatments still resulted in a robust population of high-scatter cells. Further characterization identified two high-scatter populations, labeled P1 and P2, with P2 having slightly higher forward scatter (Figure 1A, top row). Control or cells treated with LMK235 contained predominantly a P2 population, whereas panobinostat and SAHA treatments resulted in mostly P1 high-scatter cells. In parallel, we show that the P1 high-scatter population lacked MK mature markers, whereas P2 cells represented mature MKs (Figure 1A, middle row). These data indicate that inhibition of HDAC4 and HDAC5 does not impair MK differentiation in vitro, suggesting that specifically targeting HDAC4 and HDAC5 may decrease the likelihood of clinical thrombocytopenia.

Megakaryopoiesis is hyperplastic, hallmarked by an increase in cell size, shape, and DNA content (ploidy). Increasing MK ploidy coincides with an eventual increase in platelet number, with higher-ploidy MKs (normal concentration: 16 N, 32 N, and 64 N) making most of the platelets in humans [6]. We analyzed MK polyploidization following panobinostat, SAHA, and LMK235 treatments (Figure 1A, bottom row). Following differentiation, higher-ploidy MKs are clearly present in the vehicle control and LMK235-treated samples. Coinciding with the lack of mature MKs, both panobinostat and SAHA treatments significantly reduced cell ploidy, with higher-ploidy MKs (>8 N) low or not present at all with either panHDACIs (Figure 1C). These observations further substantiate that both SAHA and panobinostat impair MK differentiation.

Specific inhibition of HDAC4 and HDAC5 does not inhibit $CD34^+$ cell expansion

Next, we investigated whether HDACIs affect $CD34^+$ cell expansion and morphology during the directed differentiation processes. To address this question, we cultured $CD34^+$ cells in the presence of HDACI (500 μmol/L of SAHA, 5 nmol/L of panobinostat, or 75 nmol/L, 200 nmol/L, and 400 nmol/L of LMK235) for 8 days (which represents the middle point of the directed differentiation process) and captured images under bright-field microscopy (Figure 2A). In addition, cell numbers we quantitated by hematocytometer (Figure 2B). Initially, 30,000 cells/mL were plated and 7 hours following plating, cells were imaged as "day 0." After 8 days of directed differentiation, control cells expanded to approximately 271,000 cells/mL. SAHA significantly reduced the number of expanded cells to approximately 145,000 cells/mL. Furthermore, using 5 nmol/L panobinostat, a concentration shown to be inhibitory but not cytotoxic [4,5], dramatically reduced cell numbers to approximately 68,000 cells/mL. The reduction in cell number expansion following SAHA or panobinostat treatments coincided with an enrichment of cells with smaller sizes. Importantly, LMK235 up to 400 nmol/L (100 × of enzymatic IC_{50}) had no significant effect on cell numbers. These data suggest that specifically inhibiting HDAC4 and HDAC5 does not disrupt HSC expansion during the MK differentiation process.

Inhibition HDAC6 by tubacin has no effect on MK cell maturation

HDAC6 is a class II HDAC that specifically deacetylates acetylated tubulin. Inhibition of HDAC6 by

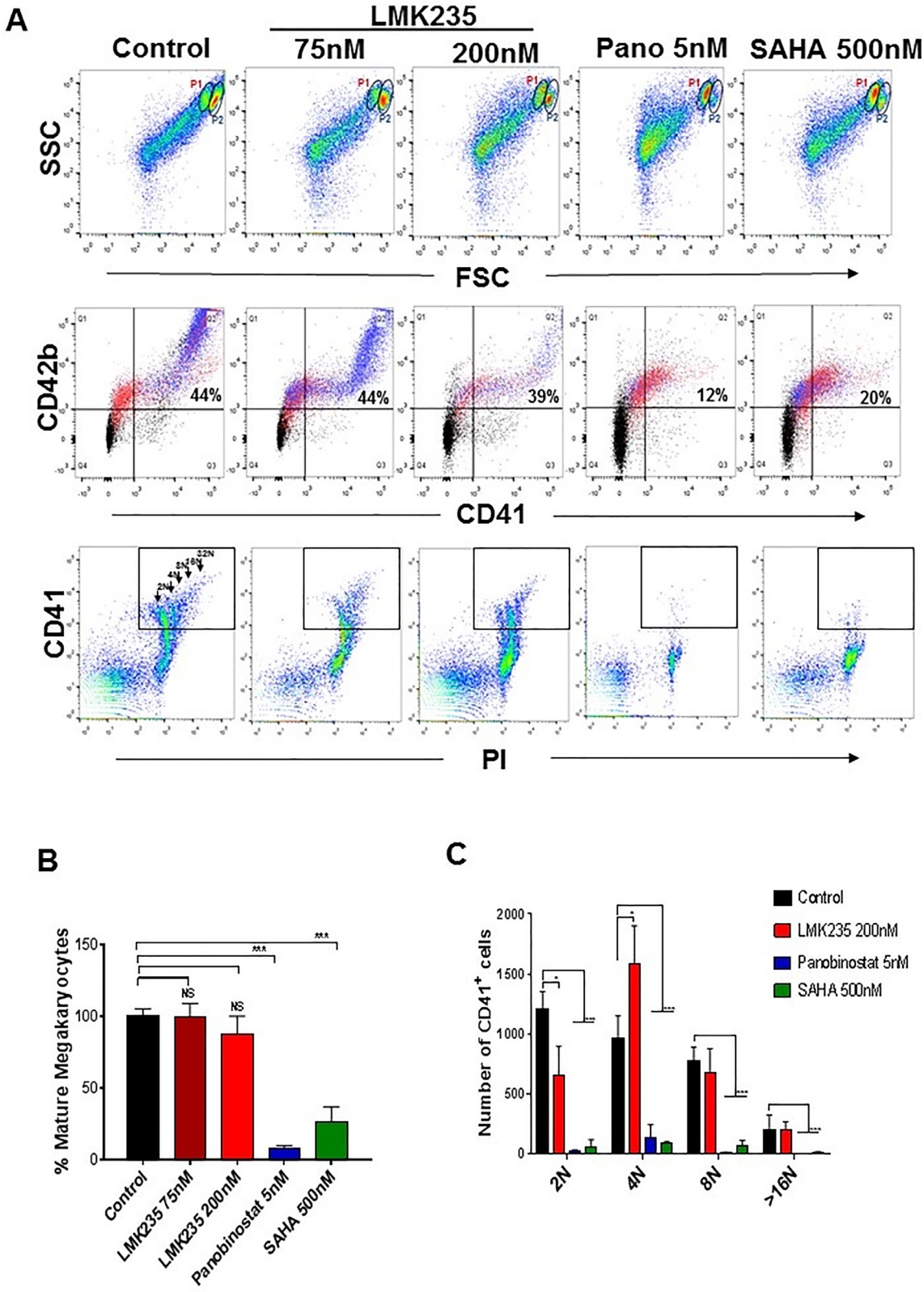

Figure 1. Specifically targeting HDAC4 and HDAC5 by LMK235 avoids impairing MK differentiation. $CD34^+$ HSC cells were cultured and induced to differentiate to MKs in the presence of 0.1% DMSO only (control), LMK235 (75 and 200 nmol/L), panobinostat (5 nmol/L), or SAHA (500 nmol/L) for 14 days, followed by fluorescence-activated cell sorting analyses. **(A)** Top row: Dot plot of forward scatter (FSC) versus side scatter (SSC) outlining MK cell size and shape, respectively. Two distinct populations (P1 and P2) of high-scatter cells were identified and

tubacin increases tubulin acetylation [12,13]. To determine whether hyperacetylation of α-tubulin (by inhibiting HDAC6 with tubacin) impairs MK maturation, we treated differentiating $CD34^+$ cells for 14 days with tubacin. Tubacin at 300 nmol/L showed no adverse effect on MK maturation (Figure 3A). The percentage of mature MKs was 47% and 48% in control and tubacin-treated cultures, respectively. In addition, the P1 high-scatter population, shown in Figure 1A to represent the majority of mature MKs, was present in the tubacin-treated cells as well. The experiment was repeated at least three times and confirmed no statistically significant difference in mature MKs following tubacin treatment. In addition, there was no difference in cell ploidy (Figure 3B), confirming that tubacin also does not affect megakaryopoiesis.

LMK235 attenuates proliferation of ovarian cancer cells

Chemotherapy is an important component of the management of ovarian cancers. To evaluate the effects of LMK235 at given doses on cancer proliferation, we treated an ovarian cancer cell line A2780 for 72 hours with LMK235, tubacin, or panHDACIs (panobinostat and SAHA) and compared their effects on cancer cell proliferation (Figure 4). After 72 hours, all tested HDACIs inhibited cancer cell proliferation rates, with potency of 200 nmol/L LMK235, >500 nmol/L SAHA, >5 nmol/L panobinostat, >75 nmol/L LMK235, and > 300 nmol/L tubacin. These data suggest that the concentrations of LMK235 used to evaluate MK maturation were biologically relevant.

GATA-1 loss, but not hyperacetylation, of α-tubulin is correlated to panHDACI-mediated impairment of MK differentiation

The mechanisms underlying clinical thrombocytopenia induced by panHDACIs remains unclear. A reduction in MK maturation caused by impairment of the GATA-1 transcriptional function [3] has been proposed, but the underlying mechanism has not been clearly delineated. To explore how inhibition of class II HDACs avoids MK differentiation impairment associated with panHDACIs, we treated Meg-01 cells for 48 hours with LMK235, panobinostat, or SAHA and investigated the effects on the acetylation status of α-tubulin and H3 and on GATA-1 protein and mRNA levels (Figures 5A and B). We observed that both panobinostat and SAHA resulted in a significant increase in acetylated α-tubulin and a profound loss of GATA-1 protein (Figure 5A). LMK235 increased α-tubulin acetylation, but did not lead to loss of GATA-1 protein levels. Similarly, tubacin strongly induced α-tubulin acetylation without a detectable decrease in GATA-1 levels. We also noted that all HDACIs tested had no significant effects on GATA-1 mRNA levels (Figure 5B), which is consistent with previously reported findings [5,11]. Both panHDACIs (SAHA and panobinostat) significantly induced H3 acetylation (Figure 5C). Although HDAC4, HDAC5, and HDAC6 mainly affect acetylation of nonhistone proteins, a slight increase in H3 acetylation has been reported [14]. Consistent with published data, a slight increase in H3 acetylation caused by LMK235 and tubacin was also observed.

To further investigate the mechanism of GATA-1 protein loss, we investigated whether the proteasome system is required for this degradation. We tested whether the proteasome inhibitor MG132 would prevent the loss of GATA-1 caused by panHDACIs (Figure 5D). We treated cells with panobinostat or SAHA for 6 hours and observed reduced levels of GATA-1 proteins; however, when cells were cotreated with MG132, GATA-1 levels remained the same or slightly increased. These data establish for the first time that GATA-1 loss caused by panHDACIs is mediated by a proteasome-dependent degradation.

Discussion

Our findings show that specifically targeting HDAC4, HDAC5, and HDAC6 may potentially avoid thrombocytopenia, a detrimental adverse effect often caused by panHDACIs. We further show that the panHDACIs panobinostat and SAHA at concentrations relevant to their clinical C_{max} impaired MK cell maturation, as noted by the reduced number of mature MKs paralleled by reduced cell ploidy. This effect appears to be in

P2 was further characterized as mature MKs, whereas P1 was mainly undifferentiated MKs. Middle row: To evaluate MK cell maturity, cells were labeled with fluorescein isothiocyanate (FITC), an anti-CD41 marker present on all MKs, and PE-anti-CD42b, a mature MK cell marker. The analytical gate was set to include only viable cells (7-AAD negative cells). Dot plot in the upper right quadrant (Q2) indicates mature, differentiated MKs. Percentages of cells are given in charts. As part of the high-scatter population characterization, P1 cell population is labeled red, the higher FSC population P2 is labeled blue, and the rest of the viable cells are labeled black. Bottom row: Cell ploidy was evaluated by staining DNA with PI and quantifying PI ploidy classes in $CD41^+$ cells. The arrows indicate ploidy classes from 2 N to >32 N ($n = 3$). **(B)** Following 14-day induced differentiation of $CD34^+$ cells, mature MKs were quantified in three independent experiments and presented as means with error bars representing standard deviations. Control samples were set as 100% and HDACI-treated cells were compared with controls. ***$p < 0.005$; NS=not significant; $n = 3$. **(C)** Cell ploidy was quantified following three independent experiments and is presented as means with error bars representing standard deviations. For each ploidy, treated samples were compared with the respective control samples. Ploidy was presented as the absolute number of $CD41^+$ cells. Following 14-day maturation, high-ploidy MKs were evident in the control and LMK235-treated samples. Treatment with panobinstat at 5 nmol/L or SAHA 500 nmol/L significantly decreased cell ploidy. *$p < 0.05$; **$p < 0.01$; ***$p < 0.005$; NS=not significant; $n = 3$.

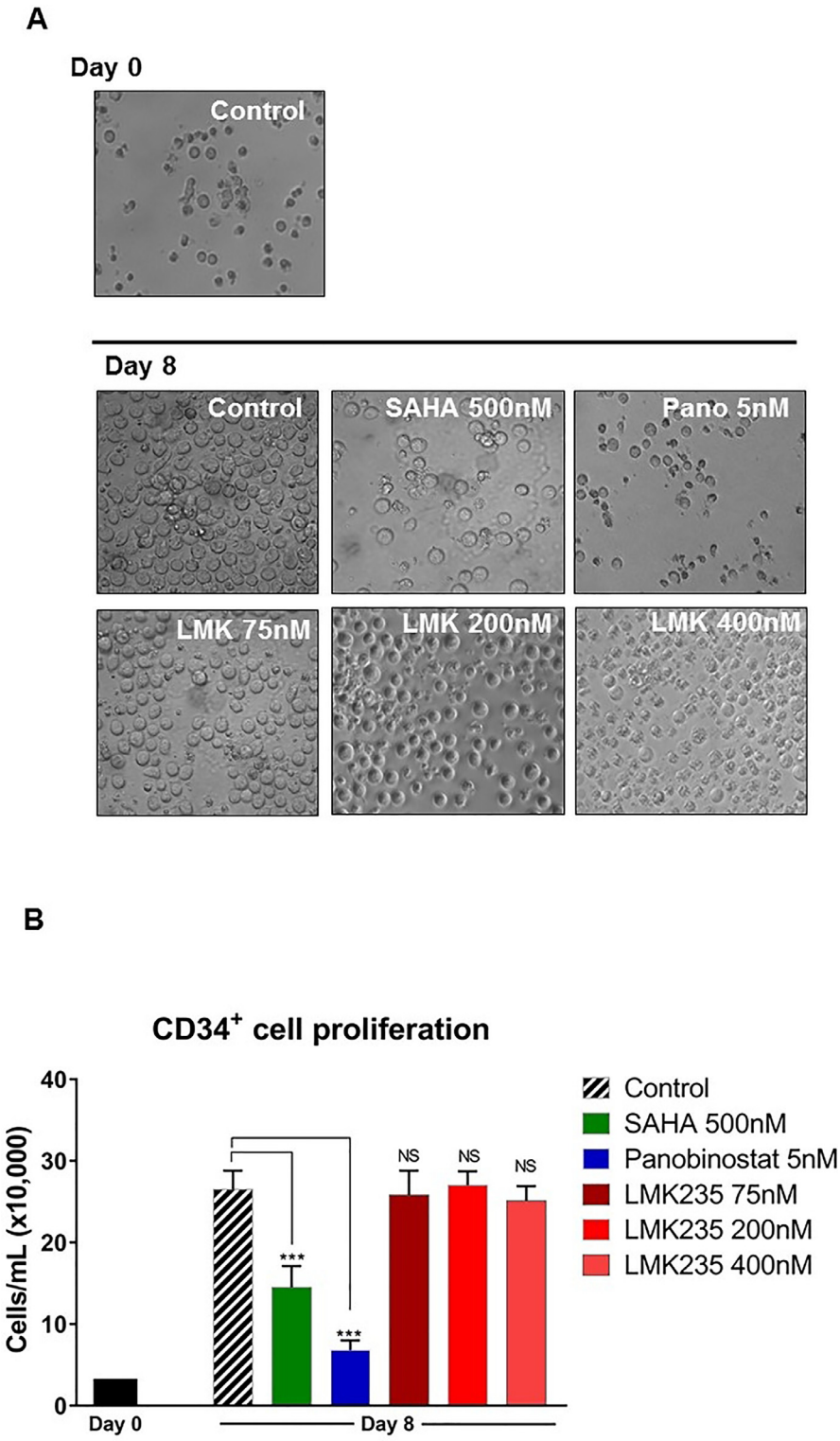

Figure 2. Effects of different HDACIs on MK cell expansion during maturation. **(A)** HSC $CD34^+$ cells were plated at 30,000 cells/mL and induced to differentiation for 8 days in the presence of 0.1% DMSO (control), LMK235, or SAHA and panobinostat as positive controls. Data indicate that LMK235 at 75, 200, and 400 nmol/L resulted in the cell number and morphology of MKs being similar to those of DMSO-treated control cells. Panobinostat treatment resulted in a significant reduction in cell number and morphologically smaller cells, indicating immature cells. Similarly, SAHA at 500 nmol/L reduced the overall number of cells; however, some large MKs were evident. Images were captured using a 40 × objective. **(B)** $CD34^+$ cells were quantified using a hemocytometer. Cells were quantified based on three independent experiments and are presented as means with error bars representing standard deviations. ***$p < 0.005$.

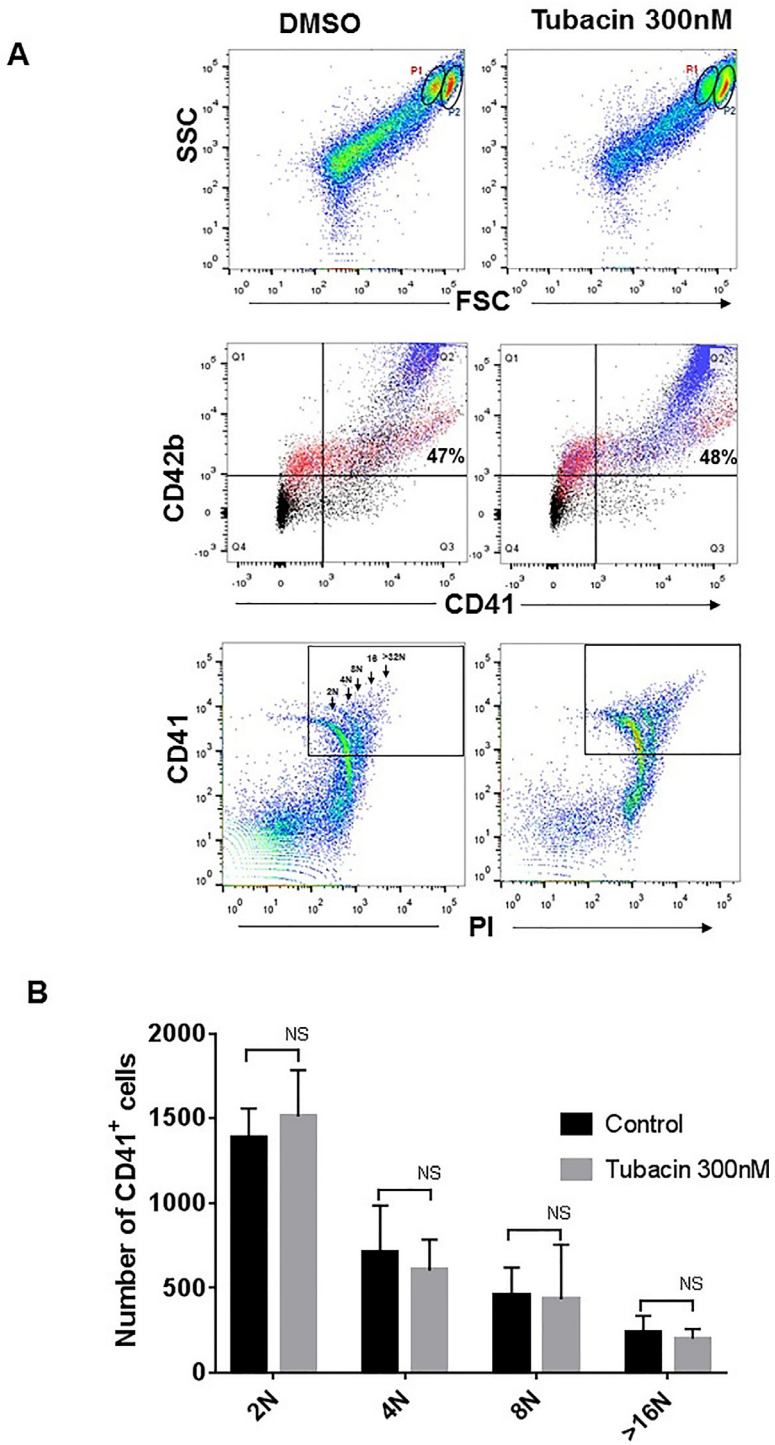

Figure 3. Tubacin does not impair MK differentiation. **(A)** Primary $CD34^+$ cells were induced to differentiate to MKs for 14 days in the presence of 0.1% DMSO (control) or tubacin at 300 nmol/L. Flow cytometric analysis was carried out subsequently. Top row: Dot plot of forward scatter (FSC) versus side scatter (SSC) outlining MK cell size and shape, respectively. Two distinct populations (P1 and P2) of high-scatter cells were identified and further characterized for MK cell maturity. Middle row: To evaluate MK cell maturity, cells were labeled with FITC anti-CD41 (a marker present on all MKs) and PE-anti-CD42b (a mature MK cell marker). The analytical gate was set to include only viable cells (7-AAD negative). Dot plot in the upper right quadrant (Q2) indicates mature, differentiated MKs. As part of the high-scatter population characterization, the P1 cell population is labeled red, the higher FSC population P2 is labeled blue, and the rest of the viable cells are labeled black. Bottom row: Cell ploidy was evaluated by staining DNA with PI and quantifying PI ploidy classes in $CD41^+$ cells. The arrows indicate ploidy classes from 2 N to >32 N. All experiments were performed three times and representative results are shown. **(B)** Cell ploidy was quantified following three independent experiments and is presented as mean with error bars representing standard deviations. For each ploidy, tubacin-treated samples were compared with the respective control samples. NS=not significant; $n = 3$.

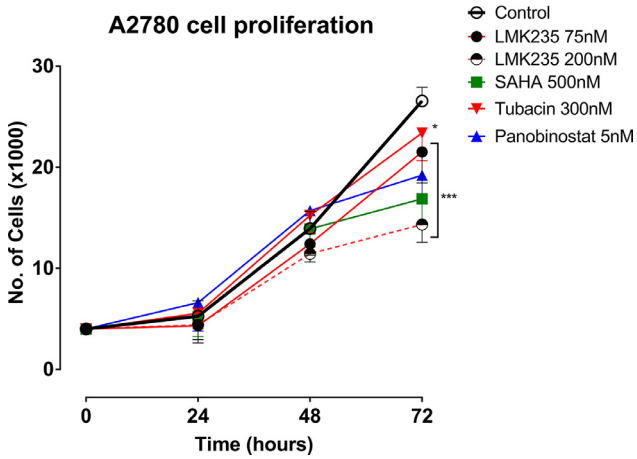

Figure 4. HDACIs inhibit ovarian cancer cell proliferation. Ovarian adenocarcinoma cells A2780 were treated for up to 72 hours with LMK235 (75 and 200 nmol/L), tubacin (300 nmol/L), SAHA (500 nmol/L), or panobinostat (5 nmol/L). Cell proliferation was quantified using CyQUANT DNA dye and is presented as absolute cell numbers based on the standard curve. Experiments were carried out with four biological repeats. $*p < 0.05$; $**p < 0.01$; $***p < 0.005$.

part mediated by the reduction in level of the GATA-1 transcription factor. We also show that GATA-1 loss, but not tubulin hyperacetylation, is critically correlated with the impairment of MK maturation. The HDAC6-specific inhibitor tubacin, which causes α-tubulin hyperacetylation but does not affect GATA-1 protein levels, had no effect on MK maturation, further supporting the notion that loss of GATA-1 protein is the underlying mechanism of panHDACI-associated thrombocytopenia. Finally, we show for the first time that the GATA-1 protein is rapidly degraded by a proteasome-dependent pathway following panHDACI treatment.

A previous study demonstrated that although panHDACIs reduce platelet numbers, they also increase bone marrow MKs in wild-type mice [4], suggesting that panHDACIs did not affect MK differentiation. However, the increase in bone marrow MKs following panHDACI treatment is likely due to the accumulation of immature MKs, cells that do not produce platelets. Follow-up studies using a more definitive $CD34^+$ maturation assay showed a clear effect of panobinostat on MK maturation [5], which is consistent with our

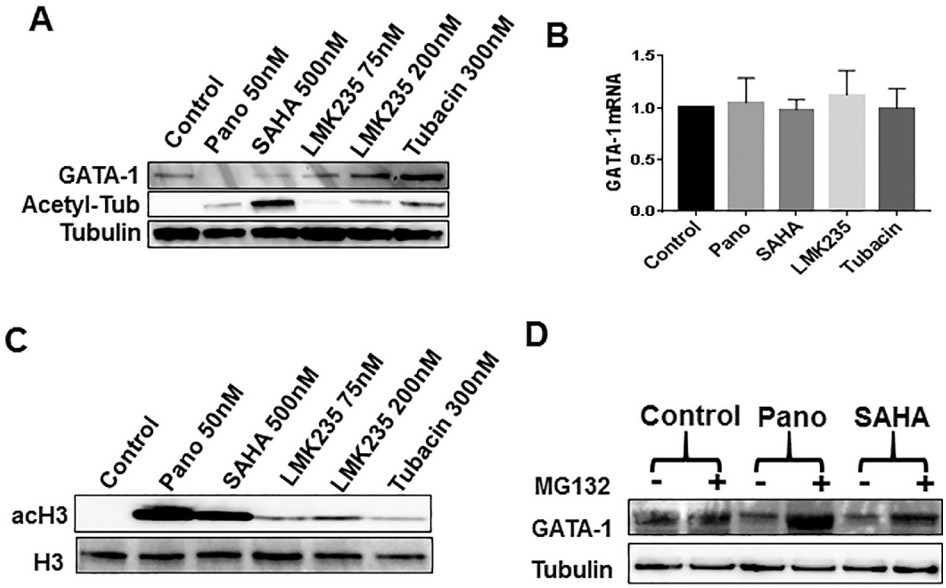

Figure 5. panHDACIs trigger proteasome-dependent GATA-1 degradation. Meg-01 cells were treated with either 0.1% DMSO or HDACIs at indicated concentrations for 48 hours and total cell lysates were prepared and examined by Western blotting analysis. **(A)** Panobinostat and SAHA reduced GATA-1 levels and increased α-tubulin acetylation. LMK235 also increased α-tubulin acetylation, but did not decrease GATA-1 levels. Similarly, tubacin increased α-tubulin acetylation, but did not suppress GATA-1 levels. Total α-tubulin levels were detected as a loading control. **(B)** Treatment with HDACIs resulted in no significant change in GATA-1 mRNA levels. Meg-01 cells were treated for 48 hours with the indicated compounds and total RNAs were extracted. GATA-1 mRNA expression levels were evaluated by qRT-PCR. ΔCt was calculated by normalized GATA-1 gene Ct values to 18S RN. **(A)** Bar graph representing the means of fold expression (compared with control) with error bars as standard deviations from three qRT-PCR reactions. **(C)** Inhibition of HDACs induces H3 acetylation. SAHA and panobinostat significantly induced histone acetylation. The HDAC class II inhibitors LMK235 and tubacin induced H3 acetylation, but at much lower intensity, consistent with the roles of class II HDACs as nonhistone deacetylases. **(D)** PanHDACI-mediated GATA-1 protein degradation is proteasome dependent. Meg-01 cells were treated for 6 hours with panobinostat (50 nmol/L) and SAHA (500 nmol/L) alone or in combination with proteasome inhibitor MG132 (5 μmol/L). Cell lysates were prepared and GATA-1 protein levels were determined by Western blot analysis.

current findings. Importantly, we show that this maturation disruption is correlated with the loss of the transcription factor GATA-1, but not α-tubulin acetylation. GATA-1 is a critical myeloid transcription factor regulating the differentiation of the MK and erythroid cell lineages. Mice and humans with GATA-1 mutations accumulate immature MK and MK-erythroid progenitors [15–17]. Earlier studies using panHDACIs noted no change in GATA-1 mRNA levels with a coinciding tubulin hyperacetylation [5], leading to the proposal that GATA-1 expression was not affected by panHDACI treatment. Our qRT-PCR-based gene expression analysis confirmed no change in mRNA levels of GATA-1. However, the protein levels of GATA-1 rapidly decreased following panobinostat or SAHA treatment, indicating that the reduction in GATA-1 levels is more likely caused by posttranscriptional mechanisms. The proteasome inhibitor MG132 blocks panHDACI-mediated loss of GATA-1 protein, suggesting that panHDACIs trigger a proteasome-dependent degradation of GATA-1. Our finding that panHDACIs cause GATA-1 degradation may explain another common adverse effect of panHDACIs, namely anemia.

Interestingly, a previous study reported that CREB-binding protein (CBP) catalyzed acetylation of GATA-1 [18], which destabilizes GATA-1 [19]. Moreover, it has been reported that panHDACIs can synergize CBP/p300-catalyzed acetylation [20]. Whether the GATA-1 destabilization caused by panHDACIs is mediated by an enhanced GATA-1 acetylation remains to be investigated.

HDAC1 and HDAC2 knockout mice have shown thrombocytopenia [21] and romidepsin, which predominantly inhibits class I HDACs, also causes thrombocytopenia [22,23], strongly indicating that the panHDACI-associated thrombocytopenia is linked to the inhibition of HDAC1 and HDAC2. In addition, an HDAC6 (class II) inhibitor, ricolinostat, was previously shown to have no effects on MK differentiation [24]

Although the class IIa members HDAC4 and HDAC5 are not essential for normal function of most somatic cells (based on mouse knockout data) [25], HDAC5 has been implicated in regulating erythropoiesis and megakaryopoiesis; its function is thought to be limited to maintaining an early progenitor pool as part of the transcriptional inhibitory complex [26–28]. However, it was also shown that, during early erythropoiesis, HDAC5 represses key hematopoietic differentiation transcription factors and keeps the cells in the progenitor state. Although erythropoiesis and megakaryopoiesis share some similarities, they differ when it comes to epigenetic transcriptional regulation. A recent report showed that the erythroid transcriptional complex NuRSERY, containing HDAC5, is present in erythroid but not in megakaryocytic lineage cells [28]. However, it was also shown that inhibition of HDAC5 had no effect on apoptosis or survival of erythroid cells, alluding to the safety of HDAC5 inhibition in hemostasis [28]. Conversely, it was shown that a reduction in HDAC5 activity was required for GATA-1-mediated hematopoiesis, leading to the hypothesis that targeting HDAC5 may actually improve hematopoiesis by stimulating differentiation of erythrocytes and MKs [26].

It has been shown that HDAC5 plays a major role in cancer stress response and survival [9,14,29,30]. Typically, HDAC5 is expressed in tissues requiring high levels of ATP (heart, neurons, and placenta) and during energy inadequate states (hypoxia, low glucose, and amino acid deprivation) [31,32]. HDAC5 overexpression was observed in a number of different tumors, suggesting a role in cancer. In tumors, cytosolic HDAC5 may act to stabilize oncogenic proteins during pervasive metabolic or chemotherapy stress [33]. We show that LMK235, at concentrations sufficient to inhibit cancer cell proliferation, resulted in no disruption of MK cell maturation. This strongly suggests that targeting HDAC5 would avoid interference with $CD34^+$ cell maturation, making HDAC5 an attractive (and safe) target in sensitizing cancer cells to metabolic stress and chemotherapy.

A recent clinical trial of the HDAC6 class II inhibitor ricolinostat, in combination with bortezomib and dexamethasone, was shown to have no negative effects on platelet formation [24]. Another study also reported that HDAC6 inhibition-induced tubulin hyperacetylation has no effect on proplatelet formation. However, the latter also reported that HDAC6 inhibition or genetic knockdown led to a strong decrease in human proplatelet formation [34]. It was proposed that the decrease in proplatelet induced by HDAC6 inhibition was attributed to cortactin hyperacetylation associated with actin disorganization, hence inducing significant changes in the distribution of MK organelles. That report highlights that the effects of HDAC inhibition on the final step of platelet formation also needs further evaluation. It should be noted that, although $CD34^+$ cell differentiation assay is a well-established approach for evaluating MK maturation in vitro, it does not evaluate platelet release from mature MKs in vivo. Nevertheless, our findings provide a rationale for in vivo studies to further address the effects of HDACIs on platelet release and clotting function.

Based on our findings and previously published reports, we outline a mechanistic explanation of panHDACI-related hematologic adverse effects and propose new strategies for cancer therapy based on selective targeting of class II HDACs, particularly HDAC4 and HDAC5 (Figure 6). We propose that HDAC1 and HDAC2 are required for MK maturation

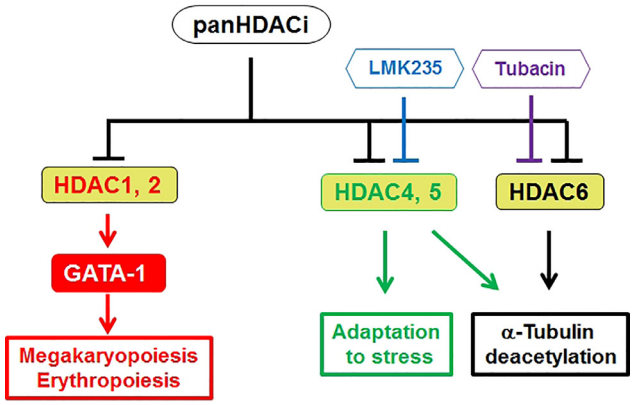

Figure 6. Effects and proposed mechanisms of cancer therapeutic HDACIs on MK differentiation. Based on current and published literature, we conclude that panHDACIs cause impairment of megakaryopoiesis mainly through the inhibition of HDAC1 and HDAC2. Because HDAC1 and HDAC2 function is required for GATA-1 stabilization, the inhibition of HDAC1 and HDAC2 leads to GATA-1 degradation, which may be mediated by GATA-1 acetylation. Compounds specifically targeting class II HDACs such as HDAC4, HDAC5, and HDAC6 avoid disrupting HDAC1/HDAC2 function, thus avoiding GATA-1 degradation and subsequent impairment of differentiation of hematopoietic progenitor cells. Therefore, specifically targeting class II HDACs as part of cancer therapy may emerge as a safer approach than nonselective HDAC inhibition.

and possibly erythropoiesis, whereas HDAC4, HDAC5, and HDAC6 are not critical for MK differentiation. Therefore, specifically targeting HDAC4 and HDAC5 as an antitumor strategy may provide clinical benefit by avoiding thrombocytopenia, a common panHDACI adverse event.

Acknowledgments

The authors thank Marry Malley and Shannon Dallas for editorial suggestions. DS would like to thank Dr. Monicah Otieno, Dr. Felice Elefant, and Dr. Tali Gidalevitz for their guidance and helpful suggestions.

Research in Dr. Sang's laboratory is supported in part by grants from the National Cancer Institute of the National Institutes of Health (R01-CA129494 to NS), Lipogen, and the State of Pennsylvania (CURE grant).

Conflict of interest disclosure

The authors declare no competing financial interests.

References

1. Oki Y, Copeland A, Younes A. Clinical development of panobinostat in classical Hodgkin's lymphoma. Exp Rev Hematol. 2011;4:245–252.
2. Giles F, Fischer T, Cortes J, et al. A phase I study of intravenous LBH589, a novel cinnamic hydroxamic acid analogue histone deacetylase inhibitor, in patients with refractory hematologic malignancies. Clin Cancer Res. 2006;12:4628–4635.
3. Matsuoka H, Unami A, Fujimura T, et al. Mechanisms of HDAC inhibitor-induced thrombocytopenia. Eur J Pharmacol. 2007;571:88–96.
4. Bishton MJ, Harrison SJ, Martin BP, et al. Deciphering the molecular and biologic processes that mediate histone deacetylase inhibitor-induced thrombocytopenia. Blood. 2011;117:3658–3668.
5. Iancu-Rubin C, Gajzer D, Mosoyan G, Feller F, Mascarenhas J, Hoffman R. panobinostat (LBH589)-induced acetylation of tubulin impairs megakaryocyte maturation and platelet formation. Exp Hematol. 2012;40:564–574.
6. Bessman JD. The relation of megakaryocyte ploidy to platelet volume. Am J Hematol. 1984;16:161–170.
7. Rubin CI, French DL, Atweh GF. Stathmin expression and megakaryocyte differentiation: a potential role in polyploidy. Exp Hematol. 2003;31:389–397.
8. Cortin V, Pineault N, Garnier A. Ex vivo megakaryocyte expansion and platelet production from human cord blood stem cells. Methods Mol Biol. 2009;482:109–126.
9. Cho Y, Cavalli V. HDAC5 is a novel injury-regulated tubulin deacetylase controlling axon regeneration. EMBO J. 2012;31:3063–3078.
10. Duvic M, Dimopoulos M. The safety profile of vorinostat (suberoylanilide hydroxamic acid) in hematologic malignancies: a review of clinical studies. Cancer Treat Rev. 2016;43:58–66.
11. Bailey H, Stenehjem DD, Sharma S. panobinostat for the treatment of multiple myeloma: the evidence to date. J Blood Med. 2015;6:269–276.
12. Zilberman Y, Ballestrem C, Carramusa L, Mazitschek R, Khochbin S, Bershadsky A. Regulation of microtubule dynamics by inhibition of the tubulin deacetylase HDAC6. J Cell Sci. 2009;122:3531–3541.
13. Siow D, Wattenberg B. The histone deacetylase-6 inhibitor tubacin directly inhibits de novo sphingolipid biosynthesis as an off-target effect. Biochem Biophys Res Comm. 2014;449:268–271.
14. Li A, Liu Z, Li M, et al. HDAC5, a potential therapeutic target and prognostic biomarker, promotes proliferation, invasion and migration in human breast cancer. Oncotarget. 2016;7:37966–37978.
15. Crispino JD, Weiss MJ. Erythro-megakaryocytic transcription factors associated with hereditary anemia. Blood. 2014;123:3080–3088.
16. Nichols KE, Crispino JD, Poncz M, et al. Familial dyserythropoietic anaemia and thrombocytopenia due to an inherited mutation in GATA1. Nat Genet. 2000;24:266–270.
17. Noh JY, Gandre-Babbe S, Wang Y, et al. Inducible Gata1 suppression expands megakaryocyte-erythroid progenitors from embryonic stem cells. J Clin Invest. 2015;125:2369–2374.
18. Hung HL, Lau J, Kim AY, Weiss MJ, Blobel GA. CREB-binding protein acetylates hematopoietic transcription factor GATA-1 at functionally important sites. Mol Cell Biol. 1999;19:3496–3505.
19. Hernandez-Hernandez A, Ray P, Litos G, et al. Acetylation and MAPK phosphorylation cooperate to regulate the degradation of active GATA-1. EMBO J. 2006;25:3264–3274.
20. Stiehl DP, Fath DM, Liang D, Jiang Y, Sang N. Histone deacetylase inhibitors synergize p300 autoacetylation that regulates its transactivation activity and complex formation. Cancer Res. 2007;67:2256–2264.
21. Wilting RH, Yanover E, Heideman MR, et al. Overlapping functions of Hdac1 and Hdac2 in cell cycle regulation and haematopoiesis. EMBO J. 2010;29:2586–2597.
22. Marson CM. Histone deacetylase inhibitors: design, structure-activity relationships and therapeutic implications for cancer. Anticancer Agents Med Chem. 2009;9:661–692.

23. Foss F, Coiffier B, Horwitz S, et al. Tolerability to romidepsin in patients with relapsed/refractory T-cell lymphoma. Biomark Res. 2014;2:16.
24. Vogl DT, Raje N, Jagannath S, et al. Ricolinostat, the first selective histone deacetylase 6 inhibitor, in combination with bortezomib and dexamethasone for relapsed or refractory multiple myeloma. Clin Cancer Res. 2017;23:3307–3315.
25. Chang S, McKinsey TA, Zhang CL, Richardson JA, Hill JA, Olson EN. Histone deacetylases 5 and 9 govern responsiveness of the heart to a subset of stress signals and play redundant roles in heart development. Mol Cell Biol. 2004;24:8467–8476.
26. Watamoto K, Towatari M, Ozawa Y, et al. Altered interaction of HDAC5 with GATA-1 during MEL cell differentiation. Oncogene. 2003;22:9176–9184.
27. Delehanty LL, Bullock GC, Goldfarb AN. Protein kinase D-HDAC5 signaling regulates erythropoiesis and contributes to erythropoietin cross-talk with GATA1. Blood. 2012;120:4219–4228.
28. Varricchio L, Dell'Aversana C, Nebbioso A, et al. Identification of NuRSERY, a new functional HDAC complex composed by HDAC5, GATA1, EKLF and pERK present in human erythroid cells. Int J Biochem Cell Biol. 2014;50:112–122.
29. Chen S, Yin C, Lao T, et al. AMPK-HDAC5 pathway facilitates nuclear accumulation of HIF-1alpha and functional activation of HIF-1 by deacetylating Hsp70 in the cytosol. Cell Cycle. 2015;14:2520–2536.
30. Guise AJ, Greco TM, Zhang IY, Yu F, Cristea IM. Aurora B-dependent regulation of class IIa histone deacetylases by mitotic nuclear localization signal phosphorylation. Mol Cell Proteomics. 2012;11:1220–1229.
31. Rutkowski DT, Kaufman RJ. A trip to the ER: coping with stress. Trends Cell Biol. 2004;14:20–28.
32. Agelopoulos K, Rohde C, Lindtner B, et al. In vivo RNAi screening identifies HDAC4 as a mediator of chemoresistance in acute myeloid leukemia. Blood. 2013;122. 1257−1257.
33. Chen S, Sang N. Hypoxia-inducible factor-1: a critical player in the survival strategy of stressed cells. J Cell Biochem. 2016;117:267–278.
34. Messaoudi K, Ali A, Ishaq R, et al. Critical role of the HDAC6-cortactin axis in human megakaryocyte maturation leading to a proplatelet-formation defect. Nat Commun. 2017;8:1786–1803.